Clipping-Enhanced Optical OFDM for Visible Light Communication Systems

Jie Lian, *Member, IEEE*, and Maïté Brandt-Pearce, *Senior Member, IEEE*

***Abstract*—Visible light communications (VLC), a new optical wireless communication technology that uses illumination light-emitting diodes as transmitters, requires a modulation scheme that is well suited to these devices' nonlinear response. Optical orthogonal frequency division multiplexing (OFDM) is a promising technique to provide high-speed data transmission for VLC. However, the peak transmitted power limitation and nonnegative transmitted signal constraint of the lighting sources can result in nonlinear signal distortion from clipping. In this paper, we propose a novel optical OFDM scheme for VLC systems called clipping-enhanced optical OFDM (CEO-OFDM) that transmits via extra time slots the information clipped by the peak power constraint. CEO-OFDM sacrifices bandwidth to allow a higher modulation index to improve the signal to noise ratio and reduce the clipping distortion caused by the peak power limitation. From analytical and numerical results, the proposed CEO-OFDM provides better bit error rate performance and higher data rate than DC-biased optical OFDM, unipolar OFDM, and asymmetrically clipped optical OFDM. Furthermore, CEO-OFDM can provide a better illumination performance that supports light dimming.**

***Index Terms*—Dimming, LED nonlinearity, optical OFDM, visible light communications.**

I. Introduction

VISIBLE light communications (VLC), a short-range optical wireless communication system using light-emitting diodes (LEDs) as transmitters has attracted much attention in recent research due to its advantages over radio-frequency (RF) communications [1]–[3]. Compared to conventional RF communications, VLC systems are immune to RF interference, have low power consumption, are safe for human health, can offer higher security, and can potentially provide high data rate transmission. Recently, an increasing number of lighting systems use LEDs as light sources due to their energy efficiency and long life expectancy. VLC systems are built on existing lighting systems using LEDs as transmitters [4]; however, LEDs are noncoherent and nonlinear optical devices with peak transmitted power and bandwidth limitations. Therefore, the characteristics of LEDs must be considered when designing a modulation scheme with high spectral efficiency for LED-based VLC systems.

Nowadays, orthogonal frequency division multiplexing (OFDM) has seen a rise in popularity for bandlimited optical systems due to its resistance to inter-symbol interference (ISI) and high spectral efficiency [5]–[9]. In conventional RF OFDM, the transmitted signals are complex valued. However, due to the noncoherent light emitted from LEDs, only intensity modulation and direct detection (IM/DD) can be used for VLC systems, which requires the transmitted signals to be real and nonnegative. Therefore, RF OFDM cannot be adopted directly in VLC systems, and OFDM has to be modified.

Many modifications to standard OFDM have been proposed for optical systems. DC-biased optical OFDM (DCO-OFDM) is one of the most commonly used optical OFDM techniques applied in VLC systems due to its simplicity [10]–[12]: a constant optical power is just added to the OFDM signal to make it nonnegative. A polar-based optical OFDM for IM/DD systems is proposed in [13], where unipolar signals are generated by transmitting the magnitude and phase information successively. Asymmetrically clipped optical OFDM (ACO-OFDM) only modulates the odd frequency subcarriers, which creates a nonnegative signal suitable for optical communications [14]. ACO-OFDM can achieve a lower peak to average power ratio (PAPR) than DCO-OFDM, and has no DC-bias requirement. A fractional reverse polarity optical OFDM (FRPO-OFDM), based on ACO-OFDM, is proposed in [15] for dimmable VLC systems. Unipolar OFDM (U-OFDM) (also known as Flip-OFDM) first transmits the positive part and then the negative part of the signal; no DC offset is required [16], [17]. Similar to U-OFDM, a non-DC biased OFDM (NDC-OFDM) is proposed to use two LEDs transmitting the positive and negative parts at the same time [18]. These OFDM techniques use Hermitian symmetry to generate real signals from the complex-valued data sequence [19]; M-ary quadrature amplitude modulation (M-QAM) is usually employed to achieve high spectral efficiency for high-speed transmission. For all of these techniques, the clipping distortion caused by the peak power limitation of LEDs degrades the system performance.

We recently proposed a clipping-enhanced optical OFDM (CEO-OFDM) for IM/DD systems in [20] in which the clipped portion of the signal is transmitted by using an extra time slot to reduce the distortion caused by the LED's limited peak transmitted power. With the help of the extra time slot, a higher received signal to noise ratio (SNR) can be achieved to support a larger QAM modulation constellation size and increase the bit rate. In

Manuscript received October 16, 2018; revised March 10, 2019 and April 12, 2019; accepted May 3, 2019. Date of publication May 7, 2019; date of current version June 5, 2019. This work was supported in part by the National Science Foundation through the STTR program under Grant 1521387 and in part by VLNComm, Inc. *(Corresponding author: Maïté Brandt-Pearce.)*

The authors are with the Charles L. Brown Department of Electrical and Computer Engineering, University of Virginia, Charlottesville, VA 22904 USA (e-mail: jl5qn@virginia.edu; mb-p@virginia.edu).

Color versions of one or more of the figures in this paper are available online at http://ieeexplore.ieee.org.

Digital Object Identifier 10.1109/JLT.2019.2915302

this paper, we expand this idea to a multi-slot CEO-OFDM that uses multiple time slots to further reduce the clipping distortion and improve the SNR. In addition, the bandwidth limiting transfer function of the LEDs, which affects the communication performance, is considered and analyzed. The proposed CEO-OFDM can provide a higher throughput than other state-of-the-art techniques. By adjusting the modulation index or adding an extra DC bias, the illumination level of CEO-OFDM can be controlled. This paper also discusses the effects of dimming on the BER performance of CEO-OFDM as compared to other OFDM techniques.

The remainder of the paper is organized as follows. Section II describes the research problem, which includes models of the nonlinearity and bandwidth limitations of LEDs, and illumination requirements for VLC systems. The principles of the proposed multi-slot CEO-OFDM and its performance are described in Section III. The effects of dimming are discussed in Section IV. The paper is concluded in Section V.

II. Problem Description

This section describes the VLC design problem addressed in this paper including the differences between RF and LED-based OFDM, nonlinearity and bandwidth limitations of LEDs, and illumination requirements of VLC systems.

A. Differences Between RF and LED-Based OFDM Systems

OFDM signals are generated by applying an inverse fast Fourier transform (IFFT) on the data stream at the transmitter and decoded using a fast Fourier transform (FFT) at the receiver. In RF systems, OFDM signals with complex values can be transmitted directly. However, only real and nonnegative signals can be transmitted in LED-based systems. Hermitian symmetry is an effective way that is commonly used to generate real-valued signals [21]. Non-negativity of the transmitted signal is accomplished in different ways in DCO-, ACO- and U-OFDM. Any remaining negative signal must be hard clipped due to IM/DD limitations.

B. Nonlinearity and Bandwidth Limitations of LEDs

LEDs working simultaneously as light sources and transmitters in VLC are driven by forward current signals. Due to the LED's structure and the lighting principles of LEDs, the output optical power and the drive current are nonlinearly related. The maximum output optical power of LEDs is limited by current saturation, resulting in clipping distortion of large-valued signals. As shown in [20, Fig. 1], the nonlinearity of the LEDs can introduce a distortion if multilevel or continuous valued signals are transmitted in VLC systems [22].

To linearize the relation between the output optical power and the input current over a range, a predistorter can be used [23]. In this paper, we assume that a predistorter is applied, and the linear range corrected by the predistorter is used to modulate the transmitted signal. The relationship between the output optical power and the input current can then be modeled as a proportional function within a finite range. The signal beyond this linear range must be hard clipped at zero and the peak power.

Due to the slow rise-time of lighting LEDs, the bandwidth of the whole VLC systems is limited by the lighting devices. In this paper, bandlimited LEDs are modeled as first order lowpass devices, and a bit loading algorithm is applied to the OFDM to optimize the throughput despite the bandlimit [24].

C. Effects of Illumination Requirements

Since VLC systems can provide illumination and wireless access simultaneously, the effects of different illumination requirements on the communication performance must be considered. According to the Illuminating Engineering Society of North America, the standard illumination level for indoor areas varies from 30 to 3000 lux based on different specific environments and functional requirements, such as in offices or hospital operating rooms [25]. During the daytime, a portion of the indoor illumination comes from sunlight; therefore, only partial illumination may need to be provided in windowed spaces by the VLC system. At night, the VLC system needs to provide full illumination to satisfy the lighting requirements. Considering the ambient light and different illumination requirements, VLC systems must be designed with a wide dynamic range for dimming control.

In VLC systems, the illumination level is determined by the average transmitted power. Therefore, unlike RF communication systems, minimizing the transmitted power is no longer a design criterion for VLC systems. Maximizing the SNR for a given average transmit power must be considered instead.

D. VLC Channel Model

The VLC channel impulse response consists of line-of-sight (LOS) and non line-of-sight (NLOS) parts. The NLOS signal is caused by reflections of the light off walls and other reflective surfaces. The impulse response of a VLC channel for a given room geometry can be simulated by using a ray-tracing algorithm [26], [27]. The intensity of the emitted light follows the Lambertain rule with a given beam-width [26]. The received power depends on the propagation distance, irradiation and incident angles, and the receiver's field of view. In this paper, the geometric model of a indoor environment is not taken into account, and only the LED frequency response and the effective received SNR is considered. The modulation design proposed and its performance analysis applies to any VLC system.

III. Multi-Slot CEO-OFDM

This section describes the principles of the proposed multi-slot CEO-OFDM scheme. We also analyze and compare the performance of multi-slot CEO-OFDM with state-of-the-art optical OFDM techniques such as DCO-, ACO-, and U-OFDM. The non-bandlimited LED case (as appropriate for emerging

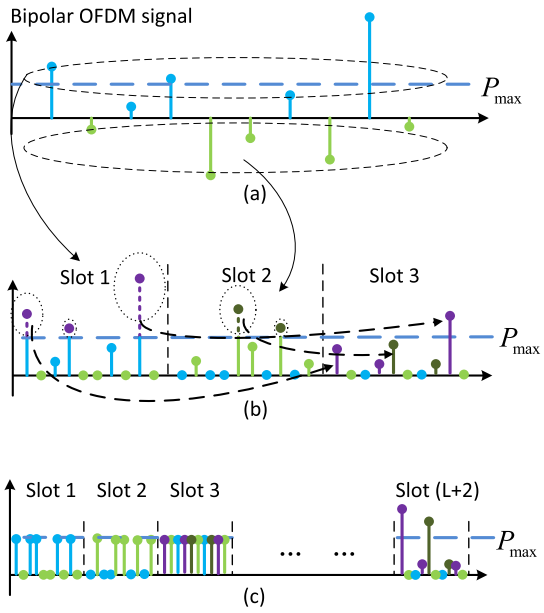

Fig. 1. Principle of multi-slot CEO-OFDM. (a) bipolar OFDM signal, (b) One-slot CEO-OFDM signal, (c) L-CEO-OFDM signal.

fast rise-time micro-LED technology) is considered first; then, the effect of the bandlimited characteristics of current lighting LEDs is discussed.

A. Transmitted Signal

Multi-slot CEO-OFDM is designed to reduce the clipping distortion by using extra time slots to transmit the clipping information, as illustrated in Fig. 1. An example of a bipolar real OFDM signal after using Hermitian symmetry is shown in Fig. 1(a). Fig. 1(b) illustrates the one-slot CEO-OFDM signal, in which positive and negative parts of the bipolar signal are transmitted successively in time slots 1 and 2, respectively. Due to the peak transmitted power constraint ($P_{\max}$), the signal amplitude larger than $P_{\max}$ in time slots 1 and 2 must be hard clipped. To reduce the clipping effects, an extra time slot (slot 3) is used to transmit the clipped information. When the modulation index of the OFDM signal is large, this third time slot can experience severe clipping. This idea is generalized to an L-slots CEO-OFDM (L-CEO-OFDM), in which L time slots (slot 3 to $L+2$) transmit the clipped signals as shown in Fig. 1(c). Clipping distortion only happens in the last slot. To guarantee the multi-slot CEO-OFDM signal can be recovered perfectly at the receiver, all the time slots should have the same duration. For a given OFDM symbol rate, a larger L results in a higher sampling rate, which is more sensitive to distortion from a sampling frequency offset (SFO). There are several methods for SFO synchronization that can be applied in the proposed L-CEO-OFDM [28]–[30]. Taking advantage of high-speed DSP, digital interpolation is an effective and efficient way for OFDM systems to mitigate the SFO effects [30]. In this paper, we assume the SFO can be eliminated.

The complexity of OFDM is based on the size of the FFT. For the proposed L-CEO-OFDM, sending extra time slots does not increase the order of complexity, which is $N \log_2 N$, where N represents the number of subcarriers. Compared with DCO- and ACO-OFDM, a buffer is needed for both U- and CEO-OFDM to construct the transmitted signal. The computational complexity of loading data onto the buffer can be ignored.

A block diagram of the proposed multi-slot CEO-OFDM transmitter is shown in Fig. 2. To simplify the notation, we analyze the signal in one OFDM symbol time. M-QAM is first applied for a high spectral efficiency. We denote the data after M-QAM for the ith subcarrier as X_i, the modulation constellation size of which is adaptively adjusted by using a bit-loading algorithm [24]. To make the transmitted signals real, X_i must be the conjugate of X_{N-1-i}, $X_{N-1-i} = X_i^*, i = 0, \ldots, N-1$, where N is the number of subcarriers.

The vector $\mathbf{X} = (X_0, X_1, \ldots, X_{N-1})^T$ is the input to an IFFT, where the output data for the kth subcarrier component, x_k, can be represented as

$$x_k = \sum_{i=0}^{N-1} X_i \exp\left(\frac{j2\pi ki}{N}\right), k = 0, 1, \ldots, N-1. \quad (1)$$

After the parallel to serial converter, the mth sample of the OFDM symbol becomes

$$x_s[m] = \frac{c}{N} \sum_{k=0}^{N-1} x_k \delta[m-k], m = 0, 1, \ldots, N-1 \quad (2)$$

where the term c is referred to as the modulation index. An example of the bipolar signal $x_s[m]$ is shown in Fig. 1(a).

The bipolar signal can be converted to a unipolar signal by flipping the negative part of $x_s[m]$ and concatenating it to the positive part of the signal. (The result of this operation is effectively a U-OFDM signal.) In this unipolar signal, the values greater than $P_{\max}$ that are clipped are saved and transmitted in subsequent time slots. Then, the clipped signal in L-CEO-OFDM can be represented as

$$x_{\text{CEO}}[m] = \underbrace{\varphi(x_s[m])}_{\text{slot 1}} + \underbrace{\varphi(-x_s[m-N])}_{\text{slot 2}} + \underbrace{\sum_{\ell=1}^{L} \varphi(|x_s[m-(\ell+1)N]| - \ell P_{\max})}_{\text{slot 3 to slot } (L+2)}$$
$$m = 0, 1, \ldots, (L+2)N-1, \quad (3)$$

where

$$\varphi(x) = \begin{cases} P_{\max}, & x \geq P_{\max} \\ x, & 0 < x < P_{\max} \\ 0, & x \leq 0 \end{cases}. \quad (4)$$

We assume $X_i, \forall i$, are independent and identically distributed (i.i.d.), and $|X_i| \leq 1$. The variance of X_i depends on the modulation constellation size for the ith subcarrier. To simplify the notation, we denote the variance of $x_k, \forall k$, as σ_d^2, which is the average variance over the samples. When N is large (usually 64 or larger), the real-valued OFDM signal $x_s[m]$ can be modeled

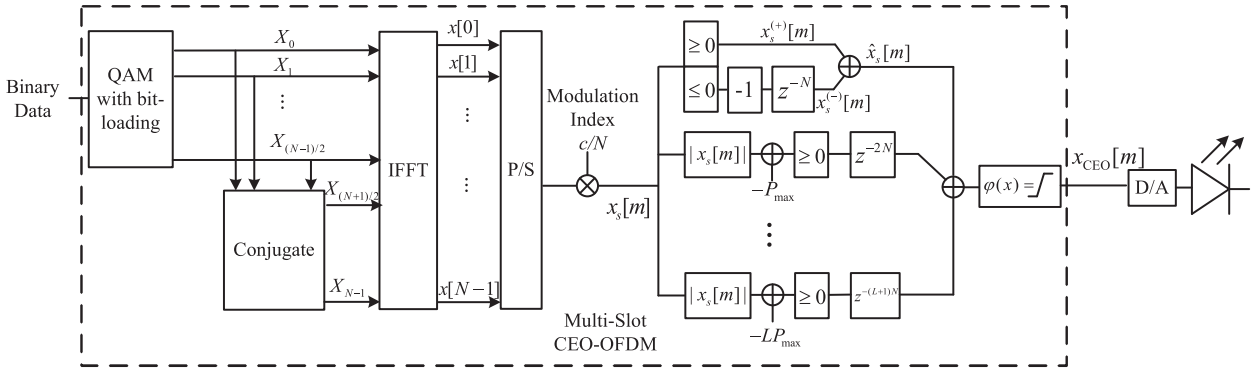

Fig. 2. Diagram of the L-CEO-OFDM transmitter with adjustable modulation index.

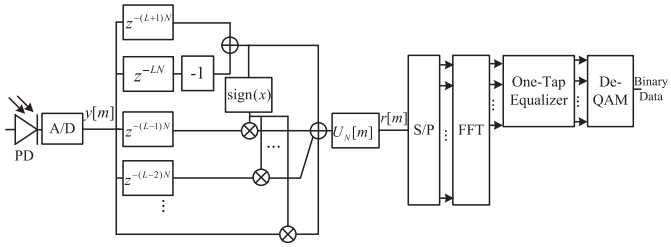

Fig. 3. Block diagram of the L-CEO-OFDM receiver.

as independent and Gaussian distributed random variables with zero mean and variance $\left(\frac{c}{N}\right)^2 \sigma_d^2$ [21].

Thus, $x_{\mathrm{CEO}}[m]$ can be modeled as a random variable with probability density function

$$f(x) = \frac{2N\left(u(x)-u(x-P_{\max})\right)}{c(L+2)\sqrt{2\pi}\sigma_d}\sum_{\ell=0}^{L}\exp\left(\frac{-N^2(x+\ell P_{\max})^2}{2c^2\sigma_d^2}\right) + \frac{\delta(x-P_{\max})}{L+2}\sum_{\ell=1}^{L+1}\mathrm{erfc}\left(\frac{\ell N P_{\max}}{c\sqrt{2}\sigma_d}\right) + \frac{\delta(x)}{L+2}\left(L+1-\sum_{\ell=1}^{L}\left(\mathrm{erfc}\left(\frac{\ell N P_{\max}}{c\sqrt{2}\sigma_d}\right)\right)\right), \quad (5)$$

where $u(\cdot)$ is the unit step function, and $\mathrm{erfc}(\cdot)$ is the complementary error function, which is defined as $\mathrm{erfc}(x) = 2/\sqrt{\pi}\int_x^\infty \exp(-y^2)\mathrm{d}y$. Note that (5) is the average probability density function over all samples, as $x_{\mathrm{CEO}}[m], \forall m$, are not i.i.d..

As shown in Fig. 2, the LED generating the transmitted optical signal is driven by an electrical current signal that is the output of a digital-to-analog (D/A) converter with $x_{\mathrm{CEO}}[m]$ as the input. For notational simplicity, in this paper we assume the LEDs have a current to optical power conversion ratio of unity.

B. Receiver Processing

The structure of the receiver for L-CEO-OFDM is illustrated in Fig. 3. The signal fed to the digital signal processor is the output of an analog to digital converter (A/D) with the signal from a photodetector as its input. The mth sample of the discrete-time version of the received signal can be modeled as

$$y[m] = \rho h[m] * x_{\mathrm{CEO}}[m] + n_y[m], \quad m = 0, 1, \ldots, (L+2)N-1 \quad (6)$$

where ρ is the responsivity of the photodetector (PD), and $n_y[m]$ is the additive noise. We assume $n_y[m]$ is Gaussian white noise with zero mean and variance that can be calculated as $\sigma_n^2 = (L+2)N_0R_s$, where R_s is the transmitted QAM symbol rate, and N_0 is the noise power spectral density. $h[m]$ is the mth sample of the discrete-time system impulse response. The operation "$*$" represents discrete-time convolution.

The received L-CEO-OFDM signal can be reconstructed into the bipolar OFDM signal by combining information of all the slots together. After the received signal is reconstructed, we can express the mth sample of the reconstructed signal in one OFDM symbol as

$$r[m] = \left(y[m]-y[m+N]\right)U_N[m] + \sum_{\ell=1}^{L}\mathrm{sign}(y[m]-y[m+N])\,y[m+(\ell+1)N]U_N[m], \quad m = 0, 1, \ldots, N-1, \quad (7)$$

where $U_N[m] = u[m] - u[m-N]$, and $u[m]$ is the discrete-time unit step function.

Due to the peak power limit of the LEDs, the reconstructed signal, $r[m]$, can be modeled by using the Bussgang theorem [21], and can be represented as

$$r[m] = \rho h[m] * \left(\alpha(c,L)x_s[m] + n_{\mathrm{clip}}[m]\right) + n_r[m], \quad (8)$$

where $\alpha(c,L)$ is a constant coefficient calculated as

$$\alpha(c,L) = \frac{1}{\sigma_x^3\sqrt{2\pi}}\int_{-\infty}^{\infty} x\psi(x,L)\exp\left(-\frac{x^2}{2\sigma_x^2}\right)dx = 1-\mathrm{erfc}\left(\frac{N(L+1)P_{\max}}{c\sqrt{2}\sigma_d}\right), \quad (9)$$

where $\psi(x, L)$ is a nonlinear function that can be represented as

$$\psi(x,L)=\begin{cases}-(L+1)P_{\max}, & x<-(L+1)P_{\max}\\ x, & -(L+1)P_{\max}<x<(L+1)P_{\max}\\ (L+1)P_{\max}, & x>(L+1)P_{\max}.\end{cases} \quad (10)$$

$n_{\text{clip}}[m]$ represents the mth sample of the clipping noise after reconstructing the data caused by the hard clipping at the transmitter. The variance of the clipping noise can be calculated as

$$\begin{aligned}&\sigma^2_{\text{clip}}(c,L)\\ &=\int_{(L+1)P_{\max}}^{\infty}\frac{2N(x-(L+1)P_{\max})^2}{c\sqrt{2\pi\sigma_d^2}}\exp\left(\frac{-N^2x^2}{2c^2\sigma_d^2}\right)dx\\ &=\frac{c(1+L)P_{\max}\sigma_d}{N\sqrt{2\pi}}\exp\left(\frac{-N^2(1+L)^2P_{\max}^2}{2c^2\sigma_d^2}\right)\\ &\quad+\frac{1}{2}\text{erfc}\left(\frac{(1+L)NP_{\max}}{c\sqrt{2\sigma_d^2}}\right)\left((1+L)^2P_{\max}^2+\frac{c^2\sigma_d^2}{N}\right).\end{aligned} \quad (11)$$

$n_r[m]$ is the additive noise on the mth sample after the reconstruction of the OFDM symbol, which is calculated as

$$\begin{aligned}n_r[m]&=(n_y[m]-n_y[m+N])\,U_N[m]\\ &\quad+\sum_{\ell=1}^{L}\text{sign}(y[m]-y[m+N])n_y[m+(\ell+1)N]U_N[m]\\ m&=0,1,\ldots,N-1.\end{aligned} \quad (12)$$

Since $n_y[m]$ is assumed to be Gaussian distributed, $n_r[m], \forall m$, are also Gaussian distributed random variables, with zero mean and variance $(L+2)\sigma_n^2$. Then, the SNR for the ith subcarrier can be calculated as

$$\begin{aligned}\gamma_i(c,L,R_s)&=\frac{c^2\alpha^2(c,L)|H[i]|^2\rho^2\sigma_d^2}{N(|H[i]|^2\rho^2\sigma^2_{\text{clip}}(c,L)+(L+2)^2N_0R_s)},\\ i&=0,1,\ldots,N-1\end{aligned} \quad (13)$$

where H is the Fourier transform of h, and $H[i]$ represents the channel frequency response for the ith subcarrier. In this paper, a one-tap equalizer at the receiver is applied to each subcarrier to compensate the phase distortion caused by the dispersive channel. Thus, given the SNR, we can approximate the bit error rate (BER) for the ith subcarrier by using the expression [31]

$$\text{BER}_i(c,L,R_s)\approx\frac{\sqrt{M_i}-1}{\sqrt{M_i}\log_2\left(\sqrt{M_i}\right)}\text{erfc}\left(\sqrt{\frac{3\gamma_i(c,L,R_s)}{2(M_i-1)}}\right), \quad (14)$$

which is a function of modulation index, c, the number of time slots used to transmit the clipped information, L, and the transmitted QAM symbol rate, R_s. M_i represents the QAM constellation size used for the ith subcarrier.

C. Performance Analysis

In this section, we analyze and compare the performance of DCO-, ACO-, U-, and multi-slot CEO-OFDM. The test environment for all techniques is the same. For DCO-OFDM, the DC offset is set to half of the peak power. However, a DC bias is not necessary for ACO-, U- and CEO-OFDM. The geometric model of the indoor environment is not considered, and only the line-of-sight (LOS) path is assumed. Unless otherwise noted, the parameters used to obtain the numerical results are shown in Table I, which is typical for indoor spaces and used as a benchmark [22]. For clarity, we first show the ideal LED case without bandwidth limitation, and then, a bandlimited LED scenario is discussed. All results shown in this paper are obtained by using the analytical expressions presented above.

TABLE I
PARAMETERS USED FOR NUMERICAL RESULTS

Responsivity, ρ	0.45 A/W
Peak optical power limit, $P_{\max}$	10 mW
Number of subcarriers, N	64
Noise spectral density, N_0	2.5×10^{-10} mW/Hz

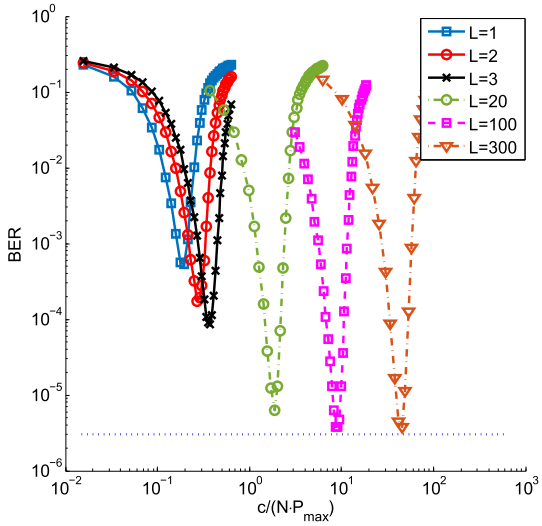

Fig. 4. BER for L-CEO-OFDM with an increasing modulation index, c/N, using 64-QAM and no bandwidth constraint. $R_s = 30$ Msps.

1) Infinite LED Bandwidth: In this section, we assume that $|H[i]| = 1, i = 0, 1, \ldots, N-1$. Therefore, the SNR for each subcarrier is assumed to be the same, i.e. $\gamma_i(c, L, R_s) = \gamma(c, L, R_s), i = 0, 1, \ldots, N-1$. To minimize the BER, an optimum modulation index, c^*, can be obtained as

$$c^*(L)=\arg\max_c\gamma(c,L,R_s). \quad (15)$$

For the proposed L-CEO-OFDM, a larger L requires more bandwidth with a fixed transmission symbol rate. When $L\to\infty$, and $c\to\infty$, the transmitted waveform only contains two values: 0 and $P_{\max}$. It is interesting to note that, for IM/DD systems, the optimum waveform must have this property if the channel capacity is achieved [32]–[34].

Fig. 4 shows the BER performance of the CEO-OFDM with different numbers of slots L for transmitting the clipped information. The modulation index, c, is adjusted to control the scale of the transmitted signal. The BER is calculated by using (13) and (14). In general, for each L, the BER performance at first improves when the modulation index increases. Then, after the clipping noise dominates, further increasing the modulation index eventually causes the BER performance to worsen. A

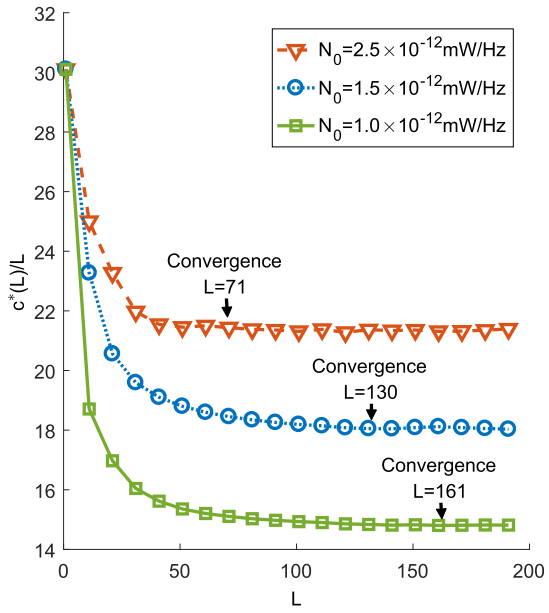

Fig. 5. Relationship between the number of slots, L, and the optimal signal scale per slot, $c^*(L)/L$, for different noise spectral density N_0.

TABLE II
OPTIMUM CLIPPING-ENHANCED SLOT NUMBER

3 dB Bandwidth	N_0=2.5×10^{-10} mW/Hz		N_0=5×10^{-10} mW/Hz	
	L^*	R_b (Mbps)	L^*	R_b (Mbps)
1 MHz	0	7.3	0	5.2
20 MHz	1	146.7	1	109.7
80 MHz	2	467.2	2	355.2
140 MHz	4	741.4	3	524.3
200 MHz	7	1065.6	6	711.2

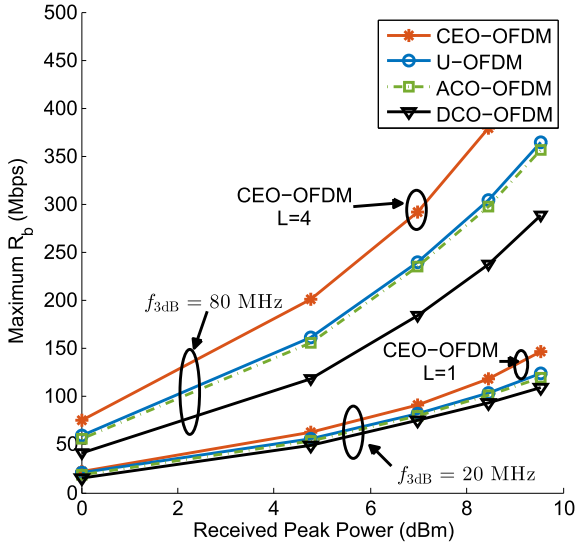

Fig. 6. Maximum bit rate comparison for different peak powers, using two bandlimited LEDs. The 3 dB bandwidths of the LEDs are 20 MHz and 80 MHz. A bit loading algorithm is used.

larger L introduces less clipping distortion, and allows the use of a larger modulation index to reach the minimum BER. The performance of L-CEO-OFDM achieves a limit as L increases, and the minimum BER eventually converges, as shown as a dotted line in Fig. 4.

Fig. 4 also shows the optimal modulation index to achieve the minimum BER for a given L. The relationship between the number of slots to transmit the clipping information, L, and its corresponding optimum modulation index $c^*(L)$, is shown in Fig. 5. For a large L, the SNR expression in (13) can be simplified as a function of c/L, R_s and N_0, which is shown in (18) and (19) in the Appendix. Since the channel capacity is limited, the SNR approaches a limit when L goes to infinity. Therefore, $c^*(L)/L$ converges to a constant, and we can predict the optimum modulation index to achieve the minimum BER for large L.

2) Finite LED Bandwidth: The bandwidth limit due to the slow rise-time of currently available lighting LEDs is a key factor affecting the VLC system throughput. In this section, we model the LED as a first order low pass device that dominates the bandwidth of the overall channel. Although the 3 dB bandwidth is limited, a bit loading algorithm and a single-tap equalizer can be implemented to effectively use a significantly broader bandwidth and improve the throughput. To make a fair comparison, we use the same bit loading algorithm and single-tap equalizer for DCO-, ACO-, U-, and the proposed L-CEO-OFDM. Since the required bandwidth increases with an increasing L for a given QAM symbol rate R_s, there exists an optimum number of extra time slots to transmit the clipped information and maximize the throughput. The optimum number of slots, L^*, and the optimum modulation constellation size for ith subcarrier, M_i^*, can be obtained by

$$[M_i^*, L^*] = \arg \max_{M_i, L, R_s} \sum_{i=0}^{(N-1)/2} R_s \log_2 M_i$$
$$\text{s.t.} \frac{\sqrt{M_i}-1}{\sqrt{M_i}\log_2\left(\sqrt{M_i}\right)} \operatorname{erfc}\left(\sqrt{\frac{3\gamma_i(c^*, L, R_s)}{2(M_i-1)}}\right) < B^{\max}, \tag{16}$$

where $B^{\max}$ is the maximum BER allowed. Since only a few values of L and M_i need to be tested, a simple brute-force method can be used to numerically solve this multivariate optimization problem.

Table II shows numerical results for the maximum throughput data rate R_b and the optimal number of time slots to transmit the clipped information for different LED bandwidths and noise levels that can result from differing levels of background light. For a wider bandwidth LED, a larger optimal number of slots can be applied to maximize the throughput, up to a point, as shown in Fig. 4. For a higher noise level, a larger L introduces a higher noise power, which degrades the system performance. Therefore, the optimal L for a higher noise level case is smaller, which is consistent with the results shown in Fig. 5.

A throughput comparison of DCO-, ACO-, U-, and L-CEO-OFDM for a bandlimited LED is shown in Fig. 6. 4-CEO-OFDM and 1-CEO-OFDM are used. According to Table II, they are

optimal for 80 MHz and 20 MHz 3 dB bandwidth LEDs, respectively, assuming the lower noise level. From this figure, L-CEO-OFDM can provide higher bit rates than DCO-, ACO- and U-OFDM even in severely bandlimited cases.

IV. CEO-OFDM Under Illumination Requirements

Illumination and dimming control are significant design factors that must be considered for VLC systems. The illumination level needs to be adjustable to satisfy different lighting requirements. Since the illumination level is proportional to the average optical power, we directly control the average optical power for dimming. In this paper, two design parameters, the modulation index and a DC bias, are used to control the dimming level. Since the effects of the LED's bandwidth does not severely affect the average optical power, we only discuss the ideal case of no bandwidth limitation (the large LED bandwidth case), for simplicity.

A. Modulation Index Selection

For L-CEO-OFDM, an increasing modulation index can increase the received average optical power. From the probability density function of the transmitted signal in the L-CEO-OFDM system given in (5), the received average optical power can be modeled as a function of the modulation index, c, and the number of slots used to transmit the clipping information, L, as

$$\begin{aligned}\bar{P}(c,L) &= \int_0^{P_{\max}^-} x\cdot f_{\mathrm{x}}(c,L,x)dx + \frac{P_{\max}}{L+2}\sum_{\ell=1}^{L}\operatorname{erfc}\left(\frac{\ell N P_{\max}}{c\sqrt{2}\sigma_d}\right)\\ &= \frac{2c\sigma_d}{N(L+2)}\left(1-\exp\left(\frac{-N^2(L+1)^2P_{\max}^2}{2c^2\sigma_d^2}\right)\right)\\ &\quad+\frac{(L+1)P_{\max}}{L+2}\operatorname{erfc}\left(\frac{N(L+1)P_{max}}{c\sqrt{2}\sigma_d}\right)\\ &\quad-\frac{P_{\max}}{L+2}\operatorname{erfc}\left(\frac{NP_{max}}{c\sqrt{2}\sigma_d}\right),\end{aligned}\tag{17}$$

where $P_{\max}^-$ is strictly less than $P_{\max}$.

A BER comparison of DCO-, ACO-, U-, and CEO-OFDM as a function of the illumination level is given in Fig. 7. In this figure, the modulation index is controlled to adjust the illumination. The results show that the minimum achieved BER of CEO-OFDM is lower than the other three optical OFDM techniques, and a larger number of slots in CEO-OFDM can provide a better BER performance. This shows that L-CEO-OFDM successfully reduces the effects of clipping distortion.

In Fig. 7 we also compare the performance of our proposed technique with a commonly used exponential companding method, here applied to U-OFDM [35]. Since an exponential function is used to compress the OFDM signal before transmission, the additive noise at the receiver is amplified when reconstructing the received signal. For the given parameters, the exponential companding PAPR reduction method performs worse than U-OFDM at low modulation indexes. When the modulation index is optimally selected to trade off the clipping distortion and

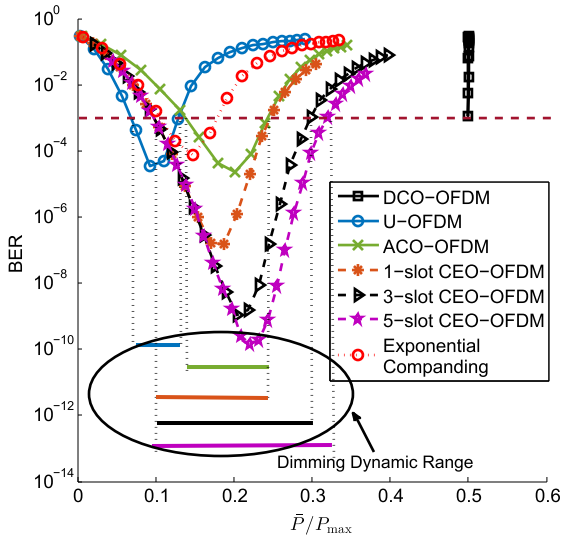

Fig. 7. Minimum BER and the corresponding average optical power, $\bar{P}$, with an increasing modulation index for DCO-, ACO-, U-, L-CEO-OFDM and exponential companding using 64-QAM. $R_s = 15$ Msps, and no bandwidth constraint.

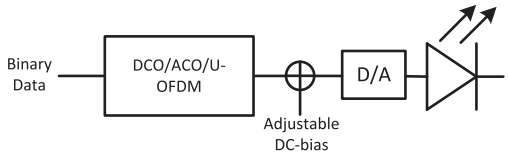

Fig. 8. Block diagram for optical OFDM techniques with an adjustable DC bias.

signal power, companding does not yield a lower minimum BER compared with uncompanded U-OFDM. This shows that reducing the PAPR by companding the transmitted signal does not provide a performance as good as the proposed CEO-OFDM.

In this paper, we define the adjustable range of illumination with corresponding BER lower than 10^{-3} as the *dimming dynamic range*. The dimming dynamic range illustrates the robustness of the VLC system to adapting to different illumination requirements. Since the average optical power for DCO-OFDM does not vary as the modulation index is adjusted, it has a zero dimming dynamic range. For all cases tested, CEO-OFDM can provide a larger dimming dynamic range than DCO-, ACO- and U-OFDM, as shown in Fig. 7. For L-CEO-OFDM, a larger dimming dynamic range can be provided by a larger L.

B. DC Bias Selection

For CEO-OFDM, a DC bias is not required to make the signal unipolar. However, we can add an adjustable DC value for illumination purposes to satisfy different illumination requirements. To make a fair comparison, we also add an adjustable DC bias to ACO-, U-, and DCO-OFDM as shown in the block diagram in Fig. 8. For CEO-OFDM, the DC bias is added to every time slot as shown in Fig. 9. The clipped information caused by the peak power constraint and DC bias can be transmitted

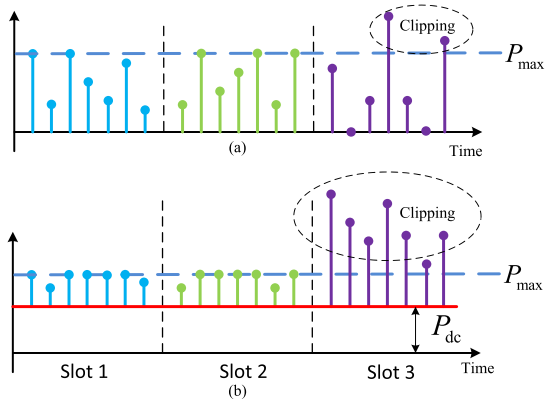

Fig. 9. Illustration of the 1-slot CEO-OFDM signal. (a) No DC bias case. (b) The case with a DC bias.

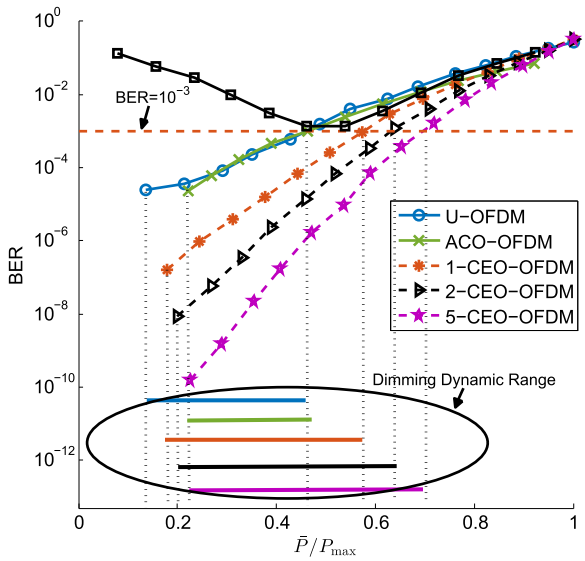

Fig. 10. Minimum BER and the corresponding average optical power with an increasing DC for DCO-, ACO-, U- and L-CEO-OFDM using 64-QAM. $R_s = 15$ Msps, and no bandwidth constraint.

via the extra time slots. Similar to the case in Section IV-A, a theoretical performance analysis of this approach, including the clipping coefficient, clipping noise variance and average optical power with an adjustable DC bias, can be derived by using the same expressions in (9), (11) and (17), respectively, replacing $P_{\max}$ with $P_{\max} - P_{\rm dc}$, where $P_{\rm dc}$ is the DC bias optical power.

Since a larger DC can introduce more clipping distortion, the adjustable bias changes the communication quality. Fig. 10 shows the best (lowest BER) performance possible for DCO-, ACO-, U-, and CEO-OFDM as a function of the average optical power resulting from adding a DC bias. The minimum BER is achieved by choosing the optimum modulation index. From the results, the BER performance of the L-CEO-OFDM is better than that of DCO-, ACO- and U-OFDM for the same illumination level. If we assume a required BER of 10^{-3}, the valid dimming dynamic range for CEO-OFDM is larger than DCO-, ACO- and U-OFDM. In addition, the larger the number of slots (L) used to transmit the clipping information in CEO-OFDM, the larger the dimming dynamic range that can be achieved.

V. Conclusion

In this paper, we propose a multi-slot clipping-enhanced optical OFDM for VLC systems. Using multiple extra time slots, the clipped information caused by the peak power limit can be transmitted and recovered, and the clipping distortion is dramatically reduced. A higher modulation index can then be used for a better BER performance. Compared with DCO-, ACO-, and U-OFDM, the proposed CEO-OFDM can achieve a lower BER or a higher bit rate than other techniques. An optimum number of slots can be obtained for a given LED bandwidth to maximize the throughput. For illumination constrained systems, CEO-OFDM can provide a wider dimming dynamic range and a better BER performance by adjusting the modulation index or adding an extra DC bias.

Appendix

This appendix gives an expression for the system SNR as a function of c/L (or, equivalently, L/c), and R_s, for a large L so that $L+2 \approx L+1 \approx L$. Substituting $\alpha(c,L)$ and $\sigma^2_{\rm clip}(c, L, P_{\rm dc})$ into (13), the SNR can be approximated as

$$\gamma_i\left(\frac{L}{c}, R_s\right) \approx \frac{S_s}{S_c + S_a}, i = 0, 1, \ldots, N-1, \tag{18}$$

where

$$S_s = |H[i]|^2 \rho^2 \sigma_d^2 \left(1 - \operatorname{erfc}\left(\frac{NP_{\max}}{\sqrt{2}\sigma_d}\left(\frac{L^2}{c^2}\right)\right)\right)$$

$$S_c = \left(\frac{L}{c}\right)\frac{N|H[i]|^2\rho^2 P_{\max}\sigma_d}{N\sqrt{2\pi}}\left(\exp\left(\frac{-N^2P_{\max}^2}{2\sigma_d^2}\left(\frac{L^2}{c^2}\right)\right)\right.$$
$$\left. + \frac{1}{2}\operatorname{erfc}\left(\frac{NP_{\max}}{\sqrt{2\sigma_d^2}}\left(\frac{L}{c}\right)\right)\left(\left(\frac{L^2}{c^2}\right)P_{\max}^2 + \frac{\sigma_d^2}{N}\right)\right)$$

$$S_a = NN_0R_s\left(\frac{L^2}{c^2}\right). \tag{19}$$

The occurrences of all c and L are encircled in the expressions, showing the functional dependence of the SNR on c/L and not c and L individually.

References

[1] T. Komine and M. Nakagawa, "Fundamental analysis for visible-light communication system using LED lights," *IEEE Trans. Consum. Electron.*, vol. 50, no. 1, pp. 100–107, Feb. 2004.

[2] T. Komine, J. Lee, S. Haruyama, and M. Nakagawa, "Adaptive equalization system for visible light wireless communication utilizing multiple white LED lighting equipment," *IEEE Trans. Wireless Commun.*, vol. 8, no. 6, pp. 2892–2900, Jun. 2009.

[3] A. Jovicic, J. Li, and T. Richardson, "Visible light communication: Opportunities, challenges and the path to market," *IEEE Commun. Mag.*, vol. 51, no. 12, pp. 26–32, Dec. 2013.

[4] J. Lian and M. Brandt-Pearce, "Multiuser MIMO indoor visible light communication system using spatial multiplexing," *J. Lightw. Technol.*, vol. 35, no. 23, pp. 5024–5033, Dec. 2017.

[5] A. Azhar, T. Tran, and D. O'Brien, "A Gigabit/s indoor wireless transmission using MIMO-OFDM visible-light communications," *IEEE Photon. Technol. Lett.*, vol. 25, no. 2, pp. 171–174, Jan. 2013.

[6] H. Elgala, R. Mesleh, and H. Haas, "Indoor optical wireless communication: Potential and state-of-the-art," *IEEE Commun. Mag.*, vol. 49, no. 9, pp. 56–62, Sep. 2011.
[7] L. Wu, Z. Zhang, J. Dang, and H. Liu, "Adaptive modulation schemes for visible light communications," *J. Lightw. Technol.*, vol. 33, no. 1, pp. 117–125, Jan. 2015.
[8] M. M. A. Mohammed, C. He, and J. Armstrong, "Performance analysis of ACO-OFDM and DCO-OFDM using bit and power loading in frequency selective optical wireless channels," in *Proc. IEEE 85th Veh. Technol. Conf.*, Jun. 2017, pp. 1–5.
[9] Q. Wang, Z. Wang, and L. Dai, "Asymmetrical hybrid optical OFDM for visible light communications with dimming control," *IEEE Photon. Technol. Lett.*, vol. 27, no. 9, pp. 974–977, May 2015.
[10] M. Zhang and Z. Zhang, "An optimum DC-biasing for DCO-OFDM system," *IEEE Commun. Lett.*, vol. 18, no. 8, pp. 1351–1354, Aug. 2014.
[11] S. D. Dissanayake and J. Armstrong, "Comparison of ACO-OFDM, DCO-OFDM and ADO-OFDM in IM/DD systems," *J. Lightw. Technol.*, vol. 31, no. 7, pp. 1063–1072, Apr. 2013.
[12] J. B. Carruthers and J. M. Kahn, "Multiple-subcarrier modulation for nondirected wireless infrared communication," *IEEE J. Sel. Areas Commun.*, vol. 14, no. 3, pp. 538–546, Apr. 1996.
[13] H. Elgala and T. D. C. Little, "Polar-based OFDM and SC-FDE links toward energy-efficient Gbps transmission under IM-DD optical system constraints," *IEEE/OSA J. Opt. Commun. Netw.*, vol. 7, no. 2, pp. A277–A284, Feb. 2015.
[14] J. Armstrong and A. J. Lowery, "Power efficient optical OFDM," *Elect. Lett.*, vol. 42, no. 6, pp. 370–372, Mar. 2006.
[15] T. Q. Wang and X. Huang, "Fractional reverse polarity optical OFDM for high speed dimmable visible light communications," *IEEE Trans. Commun.*, vol. 66, no. 4, pp. 1565–1578, Apr. 2018.
[16] D. Tsonev, S. Sinanovic, and H. Haas, "Novel unipolar orthogonal frequency division multiplexing (U-OFDM) for optical wireless," in *Proc. IEEE 75th Veh. Technol. Conf.*, May 2012, pp. 1–5.
[17] N. Fernando, Y. Hong, and E. Viterbo, "Flip-OFDM for optical wireless communications," in *Proc. IEEE Inf. Theory Workshop*, Oct. 2011, pp. 5–9.
[18] Y. Li, D. Tsonev, and H. Haas, "Non-dc-biased OFDM with optical spatial modulation," in *Proc. IEEE 24th Annu. Int. Symp. Pers., Indoor, Mobile Radio Commun.*, Sep. 2013, pp. 486–490.
[19] D. J. F. Barros, S. K. Wilson, and J. M. Kahn, "Comparison of orthogonal frequency-division multiplexing and pulse-amplitude modulation in indoor optical wireless links," *IEEE Trans. Commun.*, vol. 60, no. 1, pp. 153–163, Jan. 2012.
[20] J. Lian and M. Brandt-Pearce, "Clipping-enhanced optical OFDM for IM/DD communication systems," in *Proc. IEEE Int. Conf. Commun. Workshop*, May 2018, pp. 1–6.
[21] J. Armstrong, "OFDM for optical communications," *J. Lightw. Technol.*, vol. 27, no. 3, pp. 189–204, Feb. 2009.
[22] M. Noshad and M. Brandt-Pearce, "Hadamard-coded modulation for visible light communications," *IEEE Trans. Commun.*, vol. 64, no. 3, pp. 1167–1175, Mar. 2016.
[23] W. Xu, M. Zhang, D. Han, Z. Ghassemlooy, P. Luo, and Y. Zhang, "Real-time 262-Mb/s visible light communication with digital predistortion waveform shaping," *IEEE Photon. J.*, vol. 10, no. 3, pp. 1–10, Jun. 2018.
[24] Y. J. Zhang and K. B. Letaief, "Multiuser adaptive subcarrier-and-bit allocation with adaptive cell selection for OFDM systems," *IEEE Trans. Wireless Commun.*, vol. 3, no. 5, pp. 1566–1575, Sep. 2004.
[25] *IESNA Lighting Handbook*, 9th ed. New York, NY, USA: I.E.S. North Amer., 2000.
[26] K. Lee, H. Park, and J. R. Barry, "Indoor channel characteristics for visible light communications," *IEEE Commun. Lett.*, vol. 15, no. 2, pp. 217–219, Feb. 2011.
[27] P. Chvojka, S. Zvanovec, P. A. Haigh, and Z. Ghassemlooy, "Channel characteristics of visible light communications within dynamic indoor environment," *J. Lightw. Technol.*, vol. 33, no. 9, pp. 1719–1725, May 2015.
[28] H. Lee and J. Lee, "Joint clock and frequency synchronization for OFDM-based cellular systems," *IEEE Signal Process. Lett.*, vol. 18, no. 12, pp. 757–760, Dec. 2011.
[29] Z. Zhang, Q. Zhang, Y. Li, Y. Song, J. Zhang, and J. Chen, "A single pilot subcarrier-based sampling frequency offset estimation and compensation algorithm for optical IMDD OFDM systems," *IEEE Photon. J.*, vol. 8, no. 5, pp. 1–9, Oct. 2016.
[30] Q. Hu, X. Jin, and Z. Xu, "Compensation of sampling frequency offset with digital interpolation for OFDM-based visible light communication systems," *J. Lightw. Technol.*, vol. 36, no. 23, pp. 5488–5497, Dec. 2018.
[31] Z. Ghassemlooy, W. Popoola, and Rajbhandari, *Optical Wireless Communications: System and Channel Modeling With Matlab*. Boca Raton, FL, USA: CRC Press, 2013.
[32] A. D. Wyner, "Capacity and error exponent for the direct detection photon channel. I," *IEEE Trans. Inf. Theory*, vol. IT-34, no. 6, pp. 1449–1461, Nov. 1988.
[33] A. D. Wyner, "Capacity and error exponent for the direct detection photon channel. II," *IEEE Trans. Inf. Theory*, vol. IT-34, no. 6, pp. 1462–1471, Nov. 1988.
[34] S. Shamai, "Capacity of a pulse amplitude modulated direct detection photon channel," *IEE Proc. I—Commun., Speech Vis.*, vol. 137, no. 6, pp. 424–430, Dec. 1990.
[35] T. Jiang, Y. Yang, and Y.-H. Song, "Exponential companding technique for PAPR reduction in OFDM systems," *IEEE Trans. Broadcast.*, vol. 51, no. 2, pp. 244–248, Jun. 2005.

Jie Lian received the B.S. degree from Northwestern Polytechnical University, Xi'an, China, and the M.S. and Ph.D. degrees in electrical engineering from the University of Virginia, Charlottesville, VA, USA, in 2014 and 2017, respectively. He is currently a Research Associate with the University of Virginia. His current research interests include signal processing, wireless communications, optical communications, visible light communications, and indoor positioning.

Maïté Brandt-Pearce received the Ph.D. degree in electrical engineering from Rice University, Houston, TX, USA, in 1993. She is a Professor of electrical engineering and the Vice Provost for faculty affairs with the University of Virginia, Charlottesville, VA, USA. In addition to co-editing a book entitled *Cross-Layer Design in Optical Networks* (Springer, 2013), Springer Optical Networks Series, she has more than two hundred technical publications. Her research interests include free-space optical communications, visible light communications, nonlinear effects in fiber-optics, and cross-layer design of optical networks subject to physical layer degradations.

Dr. Brandt-Pearce had served on the editorial board of the IEEE TRANSACTION OF COMMUNICATIONS, the IEEE COMMUNICATIONS LETTERS, the IEEE/OSA JOURNAL OF OPTICAL COMMUNICATIONS AND NETWORKS and Springer *Photonic Network Communications.* She was a Jubilee Professor at Chalmers University, Sweden, in 2014. After serving as the General Chair of the Asilomar Conference on Signals, Systems & Computers in 2009, she served as the Technical Vice-Chair of GLOBECOM 2016. She was the recipient of an NSF CAREER Award and an NSF RIA. She was a co-recipient of Best Paper Awards at ICC 2006 and GLOBECOM 2012. She is a member of Tau Beta Pi and Eta Kappa Nu.